

# Fluorescent Polystyrene–Fe<sub>3</sub>O<sub>4</sub> Composite Nanospheres for In Vivo Imaging and Hyperthermia

By Donglu Shi,\* Hoon Sung Cho, Yan Chen, Hong Xu, Hongchen Gu, Jie Lian, Wei Wang, Guokui Liu, Christopher Huth, Lumin Wang, Rodney C. Ewing, Sergei Budko, Giovanni M. Pauletti, and Zhongyun Dong

Although many research programs focus on surface-functionalized quantum dots (QDs) as clinical tools to improve medical diagnosis,<sup>[1–14]</sup> the primary objective of these investigations has been imaging<sup>[3,15]</sup> and only a limited number of studies have explored other functionalities, including therapeutic treatment using hyperthermia.<sup>[16]</sup> The main purpose of this work is to present a new strategy in biomedical nanotechnology that allows simultaneous in vivo imaging and local therapy via hyperthermia. This novel concept is based on a unique nanostructure consisting of polystyrene nanospheres (PS NSs, ca. 100 nm in diameter) fabricated with a narrow size distribution that are modified by polyethylene oxide and that contain Fe<sub>3</sub>O<sub>4</sub> nanoparticles (5–10 nm) embedded in their matrices. QDs are immobilized on the surfaces of these composite NSs, facilitating fluorescent imaging. The Fe<sub>3</sub>O<sub>4</sub> nanoparticles encapsulated in the NSs respond to an external magnetic field by increasing the temperature of the surrounding environment (i.e., hyperthermia), which can be used therapeutically to treat tumor cells locally.<sup>[16–18]</sup>

A schematic representation of the nanostructure design used to produce magnetic NSs with surface-immobilized QDs

(QD–MNSs) is shown in Figure 1. The polyethylene-oxide-modified PS–Fe<sub>3</sub>O<sub>4</sub> NSs were synthesized by miniemulsion/emulsion polymerization.<sup>[19]</sup> Earlier research demonstrated that particle size critically affects the superparamagnetic state of the Fe<sub>3</sub>O<sub>4</sub> nanoparticles and must be controlled for biomedical applications.<sup>[16]</sup> However, this work was limited to the use of individual Fe<sub>3</sub>O<sub>4</sub> nanoparticles in the range 5–10 nm because of: 1) bioincompatibility in medical diagnosis and treatment; 2) aggregation of small particles that precluded homogenous dispersion in aqueous solutions; and 3) weak magnetic moments leading to insufficient heating and a low driving force required for magnetic manipulation.

The synthesis of a nanoscale spherical composite with a high fraction of magnetite in its matrix can effectively maintain considerable magnetic moments in an applied field for both hyperthermia and magnetic guiding. Immobilization of QDs on the surfaces of such MNSs introduces additional properties that are desirable for localized cancer diagnosis. First, QDs on the NS surfaces exhibit intense emission in the near-IR range of the electromagnetic spectrum, which is ideal for deep-tissue imaging.<sup>[20]</sup> Second, introduction of multivalent, surface-functionalized QDs

[\*] Prof. D. Shi  
The Institute for Advanced Materials and NanoBiomedicine  
Tongji University  
Shanghai 200092 (PR China)

Prof. D. Shi, H. S. Cho, W. Wang, and C. Huth  
Department of Chemical and Materials Engineering,  
University of Cincinnati  
493 Rhodes Hall, Cincinnati, OH 45221-0012 (USA)  
E-mail: shid@email.uc.edu

Prof. D. Shi  
Institute for Micro-Nanoscience  
and technology  
Shanghai Jiao Tong University  
Shanghai 200240 (PR China)

Prof. Y. Chen  
Key Laboratory of Nutrition and Metabolism, Institute for  
Nutritional Sciences  
Shanghai Institute for Biological Sciences, Chinese  
Academy of Sciences  
Shanghai 200031 (PR China)

Prof. H. Xu, Prof. H. Gu  
Med - X Institute, Shanghai Jiao Tong University  
Shanghai 200030 (PR China)

Prof. J. Lian  
Department of Mechanical, Aerospace &  
Nuclear Engineering  
Rensselaer Polytechnic Institute  
Jonsson Engineering Center  
Troy, NY 12180 (USA)

Prof. L. Wang, Prof. R. C. Ewing  
Departments of Geological Sciences, Nuclear Engineering &  
Radiological Sciences and  
Materials Science & Engineering  
University of Michigan  
Ann Arbor, MI 48109 (USA)

Dr. G. Liu  
Chemistry Division, Argonne National Laboratory  
Argonne, IL 60439 (USA)

Dr. S. Budko  
Ames Laboratory and Department of Physics and Astronomy  
Iowa State University  
Ames, IA 50011 (USA)

Prof. G. M. Pauletti  
James L. Winkle College of Pharmacy, University of Cincinnati  
Cincinnati, OH 45267 (USA)

Prof. Z. Dong  
Department of Internal Medicine, College of Medicine,  
University of Cincinnati  
Cincinnati, OH 45221 (USA)

DOI: 10.1002/adma.200803159

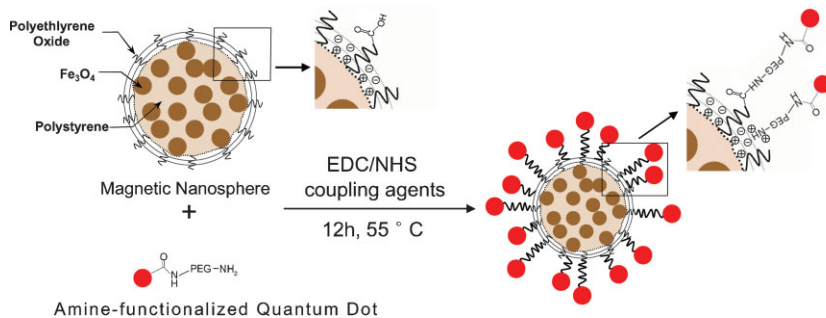


**Figure 1.** Schematic illustrating the surface-immobilized QDs on magnetic PS NSs. EDC: 1-ethyl-3-(3-dimethylaminopropyl) carbodiimide HCl; NHS: *N*-hydroxysuccinimide; PEG: polyethylene glycol.

allows coupling of unique tumor-targeting ligands, such as antibodies, increasing selectivity of this nanocomposite. Third, a high fraction of magnetite in the PS composite exhibits much stronger magnetic moments which, in contrast to individual  $\text{Fe}_3\text{O}_4$  nanoparticles, significantly improves magnetic manipulation and augments hyperthermia.

A drop of QD-MNS suspension was smeared on a glass slide for microscopic evaluation using an Olympus BX51 equipped with a fluorescence illumination module. Figure 2a shows a conventional bright-field image of QD-MNS particles without fluorescence. The QD-MNS nanoparticles are clearly visible as individual spherical units spread across the slide. Figure 2b shows the fluorescence emission of the same area shown in Figure 2a after excitation with light of wavelength,  $\lambda = 540\text{--}580\text{ nm}$  and emission at  $\lambda = 600\text{--}660\text{ nm}$ . Each particle exhibits intense red-light emission against the dark background, suggesting effective immobilization of QDs on the surfaces of the PS-MNSs. The emission behavior of the QD-MNSs was further analyzed by laser fluorescence spectrometry. The laser-excitation experiment was completed at room temperature using a 355 nm neodymium-doped yttrium aluminum garnet (Nd:YAG) pulsed laser. The spectrum of the QDs associated with the MNS surface shows a broad peak around  $\lambda = 770\text{ nm}$  (Supporting Information, Fig. S1).

The surface structures of the QD-MNSs were characterized by transmission electron microscopy (TEM) using a JEOL 2010F microscope. TEM samples were prepared by dispersing the QD-MNSs directly on holey-carbon films supported on Cu grids. Figure 3a confirms the spherical shape of the PS- $\text{Fe}_3\text{O}_4$  composite particles in the bright-field with  $\text{Fe}_3\text{O}_4$  nanoparticles (dark) embedded in the PS (light) matrix at a high concentration. High-resolution TEM imaging of the QD-MNSs (Fig. 3b) further supports the random distribution of surface-associated QDs on the composite NSs. The inset in Figure 3c is a Fourier-transformed image of a randomly selected nanoparticle, which can be indexed as ZnS. Figure 3b is the EDS spectrum, which is consistent with the chemical signals from CdSe/ZnS QDs. Combined, these data provide experimental evidence of successful immobilization of the commercial QDs onto the surfaces of the composite PS NSs.

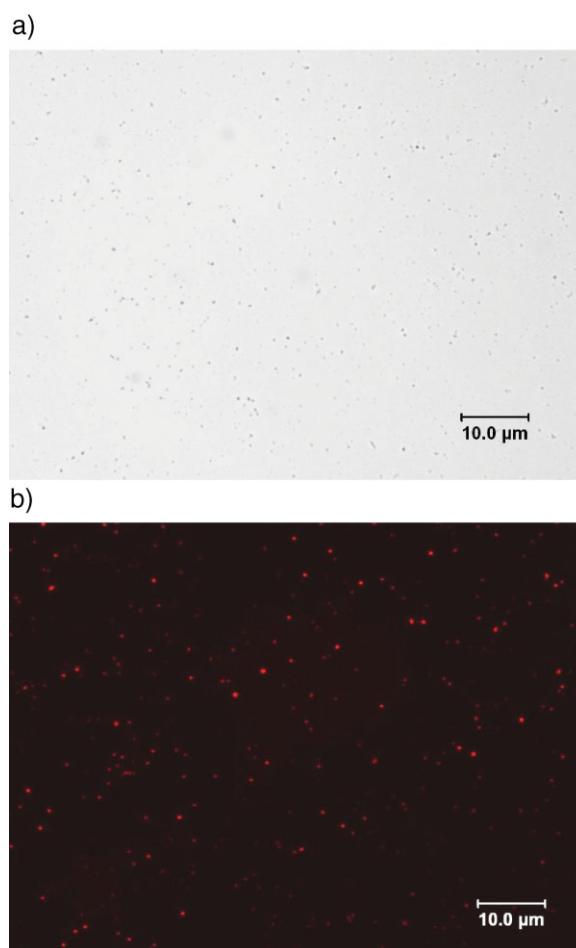
To explore potential biological applications of this novel nanocomposite, fluorescence imaging of the QD-MNSs was performed in live mice. This study was approved by the Institutional Animal Use and Care Committee (IACUC) at the

University of Cincinnati, in compliance with relevant state and federal regulations.

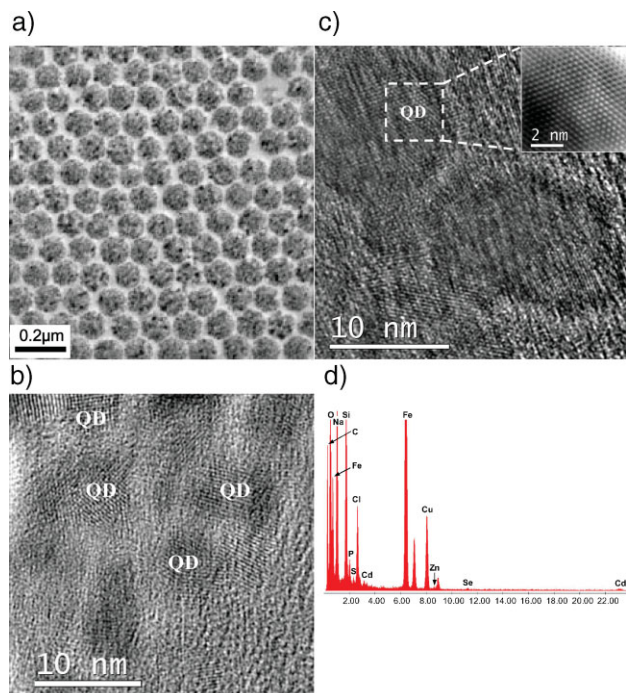
Using the Kodak Imaging station (Carestream Health, Inc., Rochester, NY; excitation: 725 nm, emission: 790 nm), in vivo fluorescence was monitored before and after intravenous injection of QD-MNSs ( $10\text{ mg mL}^{-1}$  in phosphate buffered saline (PBS),  $100\ \mu\text{L}$  of QD-MNS per animal) in nude mice via the tail vein.

Figure 4 shows the gray-scale fluorescence images from both control and QD-MNS-injected animals. The fluorescence images were acquired for 1 min. In the control, mouse autofluorescence was visible in certain ventral regions prior to QD-MNS administration (Fig. 4a). One day after injection, significant fluorescence attributed to the QD-MNSs was quantified in the anatomical region of the spleen (Fig. 4b).

The organs were harvested from the animals. As shown in insets of Figure 4a,b, ex vivo fluorescence images of the spleen indicate an accumulation of QD-MNSs in this organ of the



**Figure 2.** a) Bright-field optical image of dispersed MNSs with surface-immobilized Qdot 800 ITK amino (PEG) QDs. b) Fluorescence image of QD-MNSs obtained under excitation at 560 nm using a Texas Red emission filter set.



**Figure 3.** a) Bright-field TEM image elucidating surface structure of the QD-MNSs. b) High-resolution TEM image depicting surface properties of fabricated QD-MNSs. c) Fourier-transformed image of a randomly selected nanoparticle, which can be indexed either by hexagonal CdS or quartzite, ZnS. d) Energy dispersive X-ray (EDS) spectrum showing chemical signals of surface-associated CdSe/ZnS QDs.

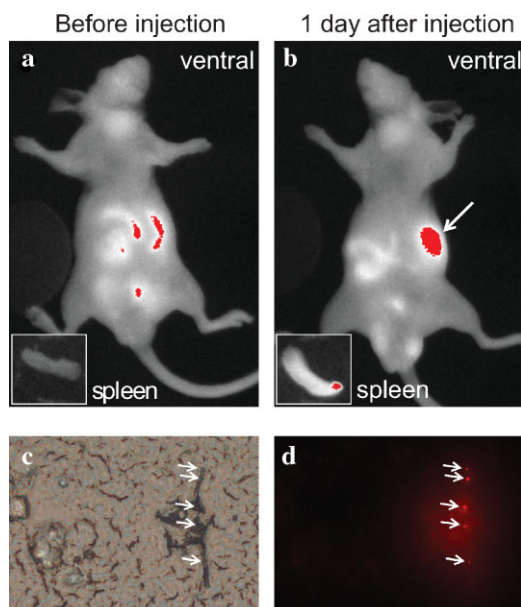


**Figure 4.** In vivo and ex vivo images after intravenous injection of QD-MNSs in nude mice. Red fluorescence signals indicate QD-MNS accumulation in the spleen; a) in vivo fluorescence before injection; b) in vivo fluorescence one day after injection; c) bright-field microscope image of a histological spleen section, and d) corresponding fluorescence image of the same section of tissue shown in (c).

treated mouse. No significant autofluorescence was measured in the untreated control animal. To support these in vivo and ex vivo images with histological evidence, tissue was embedded in optimal cutting temperature compound (EMS, Hatfield, PA), and 10  $\mu\text{m}$  cryosections were prepared at  $-20^\circ\text{C}$  using an UltraPro 5000 cryostat (Vibratome Comp., Louis, MO). Microscopic evaluation of these sections in bright-field (Fig. 4c) and fluorescence (Fig. 4d) modes confirmed the accumulation of fluorescent QD-MNSs in nonsinusoidal mouse spleen with limited distribution into red pulp reticular meshwork. These data provide clear evidence that in vivo administration of QD-MNSs results in detectable fluorescence signals in a live animal. Current research efforts focus on correlating surface properties of these novel nanocomposites with the biodistribution pattern after intravenous injection in mice using in vivo imaging.

Magnetic hysteresis and hyperthermia experiments were performed on the QD-MNSs. The hysteresis measurements show that the QD-MNSs exhibit super-paramagnetic behavior, which agrees with previously findings.<sup>[17,21]</sup> Upon applying an alternating magnetic field to the QD-MNSs, the temperature was observed to rise to  $52^\circ\text{C}$  within 30 min. These data can be found in the Supporting Information, (Fig: S2,S3).

In conclusion, based on the novel design of a nanostructure intended for simultaneous cancer diagnosis and treatment, QDs were immobilized on the surface of a superparamagnetic composite of polyethylene-oxide-modified PS NSs. The QD-MNSs exhibited strong fluorescence emission in the visible range of the electromagnetic spectrum. Images obtained from the first in vivo administration of QD-MNSs in live mice support further evaluation of this novel composite as an innovative, multifunctional nanodevice for biomedical applications. The unique combination of fluorescence emission and hyperthermia engineered into these NSs is anticipated to find clinical applications in early cancer diagnosis and tumor treatment.

## Experimental

Qdot 800 ITK amino (PEG) QDs with an emission wavelength of 800 nm were supplied by Invitrogen Corporation (Carlsbad, CA). These QD have a CdSeTe core and a ZnS shell with a covalently attached, amine-functionalized layer of PEG. The CdSeTe/ZnS QDs were dispersed in borate buffer ( $8\text{ nmol mL}^{-1}$ ). In order to assure effective surface immobilization of these QDs on the MNSs, a combined strategy of covalent coupling and electrostatic adsorption was pursued. Under physiological conditions, the positively charged amine group of the Qdot 800 ITK amino (PEG) is predicted to form electrostatically stabilized association with the electric double layer surrounding the polymer core of the MNS. Short-range, electron donor/acceptor interactions between the two surfaces are hypothesized to stabilize this association complex, which is consistent with extended DLVO (Derjaguin, Landau, Verwey, Overbeek) theory [22]. In addition, carboxyl groups resulting from auto-oxidation and partial cleavage of ethylene-oxide subunits of MNS-incorporated polysorbate [23] allow covalent coupling of the amine-functionalized QDs using conventional carbodiimide chemistry [24].

Briefly, 200  $\mu\text{L}$  of a freshly prepared solution of 30 mg NHS and 10 mg EDC in 1 mL of PBS (pH 7.4) was mixed with 100  $\mu\text{L}$  of a suspension containing 2 mg of MNSs and 160 pmol of QDs. The reaction mixture was incubated for 12 h at  $50^\circ\text{C}$ , cooled to room temperature, and centrifuged at 12 000 rpm for 5 min. The QD-MNSs were washed three times with PBS and stored in 200  $\mu\text{L}$  PBS until used.

## Acknowledgements

The work performed at University of Cincinnati (UC) was supported by a grant from the UC Institute for Nanoscale Science and Technology. The TEM analyses were conducted at the Electron Microbeam Analysis Laboratory at the University of Michigan and supported by an NSF NIRT grant (EAR-0403732). Supporting Information is available online from Wiley InterScience or from the author.

- 
- [1] D. R. Walt, *Science* **2005**, *308*, 217.
- [2] F. Mauro, *Nat. Rev. Cancer* **2005**, *5*, 161.
- [3] X. Gao, Y. Cui, R. M. Levenson, L. W. K. Chung, S. Nie, *Nat. Biotechnol.* **2004**, *22*, 969.
- [4] B. Dubertret, P. Skourides, D. J. Norris, V. Noireaux, A. H. Brivanlou, A. Libchaber, *Science* **2002**, *298*, 1759.
- [5] X. Wu, H. Liu, J. Liu, K. N. Haley, J. A. Treadway, J. P. Larson, N. Ge, F. Peale, M. P. Bruchez, *Nat. Biotechnol.* **2003**, *21*, 41.
- [6] J. K. Jaiswal, H. Mattoussi, J. M. Mauro, S. M. Simon, *Nat. Biotechnol.* **2003**, *21*, 47.
- [7] D. R. Larson, W. R. Zipfel, R. M. Williams, S. W. Clark, M. P. Bruchez, F. W. Wise, W. W. Webb, *Science* **2003**, *300*, 1434.
- [8] A. M. Derfus, W. C. W. Chan, S. N. Bhatia, *Nano Lett.* **2004**, *4*, 11.
- [9] E. B. Voura, J. K. Jaiswal, H. Mattoussi, S. M. Simon, *Nat. Med.* **2004**, *10*, 993.
- [10] S. Park, T. A. Taton, C. A. Mirkin, *Science* **2002**, *295*, 1503.
- [11] D. Shi, J. Lian, W. Wang, G. K. Liu, P. He, Z. Dong, L. M. Wang, R. C. Ewing, *Adv. Mater.* **2006**, *18*, 189.
- [12] V. Väisänen, H. Härmä, H. Lilja, A. Bjartell, *Luminescence* **2000**, *15*, 389.
- [13] W. C. W. Chan, S. M. Nie, *Science* **1998**, *281*, 2016.
- [14] X. Gao, Y. Cui, R. M. Levenson, L. W. K. Chung, S. M. Nie, *Nat. Biotechnol.* **2004**, *22*, 969.
- [15] R. Hergt, S. Dutz, R. Mueller, M. Zeisberger, *J. Phys. : Condens. Matter* **2006**, *18*, S2919–.
- [16] X. Michalet, F. F. Pinaud, L. A. Bentolila, J. M. Tsay, S. Doose, J. J. Li, G. Sundaresan, A. M. Wu, S. S. Gambhir, S. Weiss, *Science* **2005**, *307*, 538.
- [17] X. M. Wang, H. C. Gu, Z. Q. Yang, *J. Magn. Magn. Mater.* **2005**, *293*, 334.
- [18] M. Babincov, V. Altanerov, C. Altaner, P. Caronic-Caronmanec, P. Babinec, *Med. Phys.* **2004**, *31*, 2219.
- [19] H. Xu, L. L. Cai, N. H. Tong, H. Gu, *J. Am. Chem. Soc.* **2006**, *128*, 15582.
- [20] R. Weissleder, *Nat Biotech.* **2001**, *19*, 316.
- [21] P. C. Fannin, S. W. Charles, *J. Phys. D: Appl. Phys.* **1994**, *27*, 185.
- [22] J. A. Brant, A. E. Childress, *Environ. Eng. Sci.* **2002**, *19*, 413.
- [23] M. Khossravi, Y. H. Kao, R. J. Mrsny, T. D. Sweeney, *Pharm. Res.* **2002**, *19*, 634.
- [24] G. T. Hermanson, in *Bioconjugate Techniques*, Academic Press, London **1996**, pp. 8, 9.
-